Bol. Soc. Paran. Mat.
©SPM – E-ISSN-2175-1188
SPM: www.spm.uem.br/bspm

(3s.) **v. 2026 (44) 4** : 1–15.
ISSN-0037-8712
doi:10.5269/bspm.80307

Joule Heating Effects on Electromagnetic Rotating Flow of $CuO - TiO_2 - EG$ and Water Nano Liquid Over an Exponentially Stretching Surface

Mahesh Venugopalreddy, Sreegowrav Konduru Ravikumar, Dinesh Pobbathy Aswathanarayana Setty, Sibyala Vijayakumar Varma

ABSTRACT: This study investigates the heat transfer and flow characteristics of a 50%-50% ethylene glycol-water-based hybrid nanofluid, augmented with CuO (copper oxide) and TiO_2 (titanium dioxide) nanoparticles, over a rotating, exponentially stretching surface under MHD and convective boundary conditions. Using Maple, the governing equations are solved to analyze the effects of magnetic parameter (M), stretching ratio (α), rotation parameter (γ), nanoparticle volume fraction (ϕ), temperature exponent (A), and Eckert number (Ec). Results show that increasing α reduces primary flow velocity, enhances transverse velocity, and thins the thermal boundary layer. Rotation (γ) diminishes both velocity components via Coriolis effects, while a higher M reduces velocities due to Lorentz force, elevating temperatures and thermal boundary layer thickness. Increasing ϕ lowers velocities due to higher viscosity but enhances thermal conductivity, raising temperatures. A higher A reduces temperatures, thinning the thermal boundary layer, whereas elevated Ec increases temperatures via viscous dissipation. The magnetic field reduces the Nusselt number but increases skin-friction coefficients. $CuO-$based nanofluids exhibit greater magnetic sensitivity than TiO_2-based ones due to higher electrical conductivity. Hybrid nanofluids outperform conventional nanofluids in heat transfer under magnetic influence, with nanoparticle composition being critical. These findings inform applications in polymer extrusion, rotating machinery cooling, electromagnetic pumps, MHD power generation, fiber-spinning, and microchannel thermal systems, offering insights for optimizing fluid dynamics and thermal efficiency.

Keywords: Hybrid nanofluids, MHD, Joule heating, rotation, heat transfer, exponentially stretching surface.

Contents

1. Introduction

Rotating and stretching fluid flows arise in many engineering, industrial, and geophysical systems, including cooling of rotating machinery, extrusion of polymers, aerodynamic heating of turbine blades, and atmospheric circulation. Efficient heat and momentum transport in such configurations is essential for improving energy efficiency and maintaining thermal stability in advanced technologies. The interplay of rotation, stretching motion, and convective heating produces complex boundary layer structures, making these flows a subject of continuous research in modern fluid dynamics. To improve heat transfer in industrial systems, nanofluids –base fluids with dispersed nanoparticles – were introduced by Choi [3]. The study of rotating boundary layers began with the pioneering work of Wang [21] on rotating boundary layers and investigated extending a surface in a rotating fluid. Zaimi et al. [22] considered the viscoelastic behaviour of rotating fluids over stretched surfaces, illustrating how non-Newtonian effects modify flow characteristics. Javed et al. [4] extended the rotating model to exponentially stretching surfaces, a configuration relevant to real-world processes like fibre spinning and extrusion. Rosali et al. [13] studied the same model under shrinking conditions and observed boundary layer separation at certain parameter thresholds.

2020 *Mathematics Subject Classification:* 76-xx,76Bxx.
Submitted November 22, 2025. Published February 26, 2026

Thumma et al. [15], Thumma & Mishra [16]; Thumma et al. [17], Thumma & Satya [18] examined MHD nanofluid flows with heat generation, radiation, and Joule heating and observed that increasing magnetic field strength thickens the thermal boundary layer but reduces fluid velocity. Rafique et al. [10] examined hybrid nanofluid flow over an exponentially stretching sheet, focusing on entropy generation influenced by Joule-heating and couple stresses. The Power-law fluid's rotational flow is studied by Kumari et al. [5] across a stretching surface.

The investigation of Magnetohydrodynamics effects in unsteady rotating flows is done by Takhar et al. [14] and showed how magnetic fields can modify momentum and thermal layers. Many researchers Abbas et al. [1], Anwar et al. [2] have performed experimental studies to examine the HNFs viscosity and thermal conductivity. Mahmood et al. [7] has analysed mixed convection stagnation-point flow of hybrid nanofluids over sheets with variable thermal conductivity and slip conditions, underscoring the combined effect of MHD and convective heat flux conditions. Marzougui et al. [8] analysed entropy generation in MHD nanofluid systems, linking magnetic strength to energy losses. Their findings highlight the importance of balancing magnetic field benefits with associated resistive losses. Studies by Wakif et al. [20] incorporated Joule heating in hybrid nanofluid MHD flow and observed enhanced thermal stability and more uniform temperature fields in the boundary layer region. These results are essential for systems like MHD pumps and microchannel coolers, where accurate thermal modelling is critical.

Rashid et al. [11] has examined mixed convection MHD hybrid nanofluid (TiO_2–$GO/water$) between rotating discs, incorporating Joule heating, chemical reactions, and radiation. They observed that magnetic fields increase boundary layer thickness, reduce velocity, and modulate heat transfer rates. Madiha Takreem et al. [6] applied response surface methodology (RSM) to study MHD hybrid nanofluid flow over a porous exponentially stretching sheets with multiple slips. Their model accounted for Joule heating and optimized thermal performance. Rafique et al. [10] has analysed how Entropy generation occurs in an $Al_2O_3 - Cu/H_2O$ hybrid nanofluid subjected to a non-axisymmetric stagnation-point flow, where both Joule heating and viscous dissipation contribute to the thermal irreversibilities. Reddy et al. [12] explored Casson nanofluid MHD flow over a nonlinearly stretching surface, including absorption, radiation, and Joule heating. The study quantified how resistive heat generation affects thermal gradients and skin friction.

Hybrid nanofluids are synthesized by incorporating two or more distinct types of nanoparticles into a single base fluid. This combination often leads to synergistic effects, enhancing thermal conductivity and heat transfer capabilities beyond what can be achieved with single-nanoparticle nanofluids. Nowadays, researchers have explored various combinations of nanoparticles, such as Copper-Alumina ($Cu - Al_2O_3$), Carbon Nanotubes (CNTs), and metallic oxides, suspended in base fluids like water, ethylene glycol, or oil. Joule heating-also known as Ohmic heating-arises from the electrical resistance within the fluid due to the applied magnetic field. It contributes directly to the energy equation as a volumetric heat generation term. This is particularly important in high magnetic-field scenarios where resistive heating becomes non-negligible.

In systems where the working fluid is electrically conducting, applying a magnetic field induces the Lorentz force, which acts perpendicular to both the velocity and the magnetic field vectors. This force introduces resistance to the flow and depending on its magnitude, it can either stabilize or slow down the fluid motion.

The study of fluid flow over rotating and stretching surfaces has attracted increasing attention due to its extensive applications in industrial and geophysical processes, including rotating machinery, extrusion of polymers, cooling of metallic sheets, centrifugal filtration, aerodynamic heating, and magnetohydrodynamic (MHD) power generation. Nabwey et al. [9] has analysed hybrid nanofluid flow over a porous stretching cylinder, exploring thermal stratification and Joule heating effects.

A careful review of the literature reveals that the combined influence of rotation, exponential stretching, hybrid nanoparticles, magnetic fields, and convective boundary conditions has not yet been comprehensively analysed. To address this, the present study performs a Joule heating effects on electromagnetic rotating flow of $CuO - TiO_2 - EG$ and Water nano liquid over an exponentially stretching surface. A hybrid base fluid consisting of CuO and TiO_2 nanoparticles dispersed in an ethylene glycol-water mixture is considered. Using similarity transformations, the governing three-dimensional equations are reduced to ordinary differential equations and solved via Maple. The analysis focuses on the effects of stretching

ratio, rotation parameter, magnetic parameter, nanoparticle volume fraction, convective parameter, and temperature exponent on velocity distribution, temperature profile, skin friction, and Nusselt number. This work provides new insights into the coupled effects of MHD forces and hybrid nanofluids in rotating exponential stretching systems, offering valuable guidance for applications in thermal management, material processing, and magnetohydrodynamic energy systems.

2. Problem Formulation

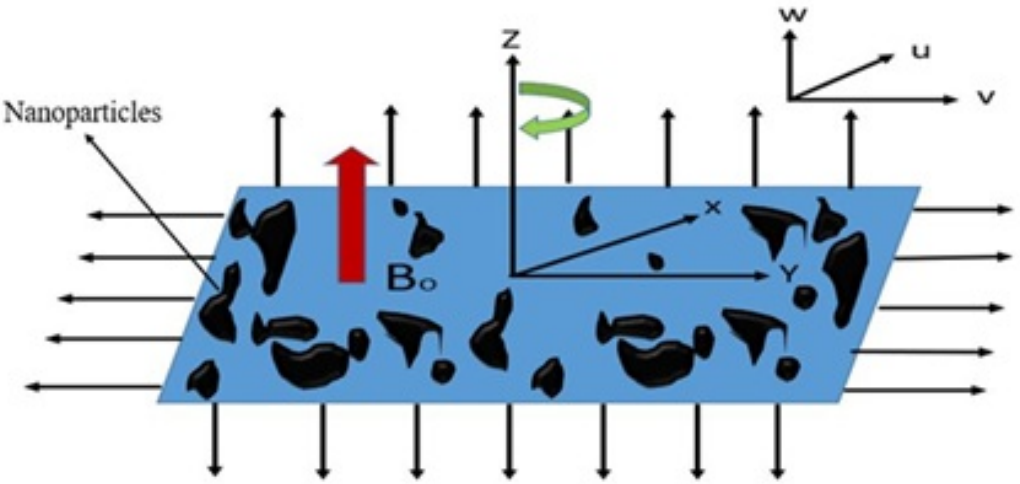

Figure 1: Schematic diagram of the flow domain.

The physical configuration of the present work is illustrated in Figure 1. We examine a rotating flow in a three-dimensional domain of electrically conducting viscous nanofluid, which is in a steady, incompressible condition, above a stretchy surface within the region $z \geq 0$, considering the influence of magnetic effects. The surface is assumed to stretch exponentially in the directions of u_w and v_w while rotation of fluid is about z-axis with a constant angular velocity. The base Nano fluid is formulated by dispersing copper oxide (CuO) and titanium dioxide (TiO_2) nanoparticles composed of an equal mixture of ethylene glycol and water in a ratio of (50 : 50). The nanofluid flow is assumed to imitate a slightly expanding exponential layer. Employing the boundary layer approximations and neglecting the effects of pressure gradient and viscous dissipation, the 3 dimensional governing equations are given by,

$$\frac{\partial u}{\partial x} + \frac{\partial v}{\partial y} + \frac{\partial w}{\partial z} = 0, \tag{2.1}$$

$$u\frac{\partial u}{\partial x} + v\frac{\partial u}{\partial y} + w\frac{\partial u}{\partial z} - 2\Omega v = \frac{\mu_{nf}}{\rho_{nf}}\frac{\partial^2 u}{\partial z^2} - \frac{\sigma_{nf}{B_0}^2 u}{\rho_{nf}} \tag{2.2}$$

$$u\frac{\partial v}{\partial x} + v\frac{\partial v}{\partial y} + w\frac{\partial v}{\partial z} + 2\Omega u \quad = \frac{\mu_{nf}}{\rho_{nf}}\frac{\partial^2 v}{\partial z^2} - \frac{\sigma_{nf}{B_0}^2 v}{\rho_{nf}} \tag{2.3}$$

$$u\frac{\partial T}{\partial x} + v\frac{\partial T}{\partial y} + w\frac{\partial T}{\partial z} \quad = \alpha_{nf}\frac{\partial^2 T}{\partial z^2} + \frac{\sigma_{nf}{B_0}^2\left(u^2+v^2\right)}{\left(\rho c_p\right)_{nf}} \tag{2.4}$$

The thermophysical properties of nano-fluids are given by :

$$\begin{aligned}
(\rho)_{nf} &= \rho_f (1-\phi) + \phi\rho_s, \\
\mu_{nf} &= \frac{\mu_f}{(1-\phi)^{2.5}}, \\
\alpha_{nf} &= \frac{k_{nf}}{(\rho C_p)_{nf}}, \\
(\rho C_p)_{nf} &= (\rho C_p)_f (1-\phi) + (\rho C_p)_s,
\end{aligned} \tag{2.5}$$

Here, μ_{nf} indicates for dynamic viscosity, ρ_{nf} stands density, α_{nf} shows thermal diffusivity, k_{nf} mentions thermal conductivity and $(\rho C_p)_{nf}$ is heat ability of nanofluid.
The above equations (2.1) to (2.5) are subjected to boundary conditions as follows,

$$\begin{aligned}
&u = u_w\ , v = v_w, w = 0, -k_{nf}\frac{\partial T}{\partial z} = h_f (T_w - T)\ ,\ at\ z = 0 \\
&u \to 0, v \to 0, T \to T_\infty,\quad as\ z \to \infty
\end{aligned} \tag{2.6}$$

Wall temperature and exponentially stretching velocities at the surface is defined as follows

$$T_w = T_\infty + T_o e^{\frac{A(x+y)}{2L}}, u_w = u_o e^{\frac{x+y}{L}},\ v_w = v_o e^{\frac{x+y}{L}}. \tag{2.7}$$

By using similarity functions are

$$\begin{aligned}
u &= u_o e^{\frac{x+y}{L}} p'(\eta), \\
v &= u_o e^{\frac{x+y}{L}} q'(\eta), \\
w &= -\Big(\frac{\upsilon u_o}{2L}\Big)^{\frac{1}{2}} e^{\frac{x+y}{2L}} (p + \eta p' + q + \eta q')
\end{aligned} \tag{2.8}$$

$$\begin{aligned}
T &= T_\infty + T_0 e^{\frac{A(x+y)}{2L}} \theta\ (\eta), \\
\eta &= -\Big(\frac{u_o}{2\upsilon L}\Big)^{\frac{1}{2}} e^{\frac{x+y}{2L}} z.
\end{aligned} \tag{2.9}$$

Here, η represents the similarity variable,T_w denotes the wall temperature, and T_∞ corresponds to the ambient fluid temperature. The continuity equation shows that it satisfies the equation after introduction of similarity transformation. Applying similarity transformation to equations (2.1) to (2.6), the momentum and energy equations are reduced to the following dimensionless forms:

$$\frac{L_1}{L_2}p''' + p''(p+q) - 2p'(p'+q') + 4\gamma q' - \frac{L_3}{L_2}Mp' = 0 \tag{2.10}$$

$$\frac{L_1}{L_2}q''' + q''(p+q) - 2q'(p'+q') - 4\gamma p' - \frac{L_3}{L_2}Mq' = 0 \tag{2.11}$$

$$\frac{1}{P_r}\frac{L_4}{L_2L_5}\theta'' - A(p'+q')\theta + (p+q)\theta' + \frac{L_3}{L_5L_2}E_cM\left(p'^2 + q'^2\right) = 0. \tag{2.12}$$

$$\begin{aligned}
\text{where}\quad L_1 &= \frac{\mu_{nf}}{\mu_f}, L_2 = \frac{\rho_{nf}}{\rho_f}\ , \gamma = \frac{\Omega_o L}{u_o}\ ,\ P_r = \frac{(\mu C_p)_f}{k_f}, \\
L_3 &= \frac{\sigma_{nf}}{\sigma_f} = \left(1 + \frac{3\left(\frac{\sigma_s}{\sigma_f} - 1\right)\emptyset}{\left(\frac{\sigma_s}{\sigma_f} + 2\right) - \left(\frac{\sigma_s}{\sigma_f} - 1\right)\emptyset}\right), \\
L_4 &= \frac{k_{nf}}{k_f} = \frac{(k_s + 2k_f) - 2\emptyset(k_f - k_s)}{(k_s + 2k_f) + \emptyset(k_f - k_s)}, L_5 = \frac{(C_p)_{nf}}{(C_p)_f}, \\
M &= \frac{\sigma_f {B_0}^2 L}{\rho_f u_0},\quad E_c = \frac{{u_o}^2}{(C_p)_f (T_w - T_\infty)}.
\end{aligned} \tag{2.13}$$

The transformed boundary conditions are

$$\begin{aligned} &p(0)=0, p'(0)=1, q(0)=0, q'(0)=\alpha,\ \theta'(0)=-\frac{N_c}{L_4}(1-\theta(0)) \quad as \quad \eta\to 0 \\ &p'\to 0,\quad q'\to 0, \theta\to 0, as\ \ \eta\to\infty \end{aligned} \tag{2.14}$$

$$\text{where}, \alpha=\frac{v_0}{u_0}, \qquad N_c=\frac{h_f}{k_f}\sqrt{\frac{2\nu_f L}{u_0}}\, e^{-\left(\frac{x+y}{2L}\right)}. \tag{2.15}$$

The equations describing skin friction coefficient and the Nusselt number are shown below,

$$C_{fx}=\ \frac{\tau_{wx}}{\frac{1}{2}\rho_f {u_w}^2}, C_{fy}=\ \frac{\tau_{wy}}{\frac{1}{2}\rho_f {u_w}^2}, N_{ux}=\ \frac{xq_w}{k_f\left(T_w-T_\infty\right)}. \tag{2.16}$$

The expressions for heat flux q_w and wall shear stresses τ_{wx}, τ_{wy} are

$$q_w=-k_{nf}\left(\frac{\partial T}{\partial z}\right)_{z=0},\ \tau_{wx}=\mu_{nf}\left(\frac{\partial u}{\partial z}\right)_{z=0},\ \tau_{wy}=\mu_{nf}\left(\frac{\partial v}{\partial z}\right)_{z=0}. \tag{2.17}$$

Apply Equations (2.8-2.9) and (2.17) in equation (2.16). The transformed equation is given by

$$\frac{1}{\sqrt{2}}C_{fx}\left(Re_x\right)^{\frac{1}{2}}=L_1 p''(0), \frac{1}{\sqrt{2}}C_{fy}\left(Re_x\right)^{\frac{1}{2}}=L_1 q''(0), \sqrt{2}\frac{L}{x}Nu_x\left(Re_x\right)^{-\frac{1}{2}}=-L_4\theta'(0). \tag{2.18}$$

Table 1: Thermophysical characteristics of nanoparticles and hybrid base fluid.

Physical Properties	$\rho\left(\frac{kg}{m^3}\right)$	$c\rho\left(\frac{J}{Kg.K}\right)$	$K\left(\frac{w}{m.K}\right)$	$\sigma\left(\frac{S}{m}\right)$
$C_2H_6O_2-H_2O$	1063.8	3630	0.387	9.75×10^{-4}
CuO	6500	540	18	2.6×10^{-8}
T_iO2	4250	686.2	8.9538	10^{-10}

3. Solution Methodology

The nonlinear boundary value system given in equations (2.10)–(2.12) is converted into a set of first-order initial value problems by introducing suitable auxiliary variables. The missing initial conditions are approximated using the shooting technique. To ensure that the far-field boundary conditions are satisfied, the similarity variable is truncated at a finite value, with $\eta_\infty=5$ found sufficient to capture the asymptotic behaviour across all parameter ranges studied. Numerical simulations are carried out in Maple with a step size of $\Delta\eta=0.001$ and a convergence tolerance of 10^{-6}. The adopted scheme, possessing a sixth-order truncation error, provides improved accuracy and computational efficiency relative to several conventional numerical approaches.

4. Results and Discussions

The present work examines the impact of velocity components in direction of $p\prime(\eta)$ and $q\prime(\eta)$, alongside the temperature distribution $\theta(\eta)$, influenced by critical parameters such as the stretching ratio (α), volume fraction (ϕ), rotation parameter (γ) and temperature exponent (A) for copper oxide (CuO) and titanium dioxide (TiO_2) nanoparticles. The graphical results are presented to highlight the combined impact of these parameters. Figures 2-4 provide the visual interpretation of these findings.

The stretching ratio parameter α exerts a significant influence on the velocity field in both streamwise and transverse directions as shown in Figure (2a-2b) and Figure (3a-3b). As α increases, the surface undergoes more rapid stretching, which intensifies the shear drag imparted to the fluid near the wall. This enhanced shear effect dissipates momentum within the boundary layer, causing the streamwise velocity component to diminish more rapidly with distance from the sheet. Consequently, the primary velocity boundary layer becomes thinner, reflecting the reduced penetration of fluid momentum away from the surface. In contrast, the transverse velocity component exhibits the opposite behaviour. The

stronger stretching in the streamwise direction induces a compensatory cross-flow through the continuity requirement, thereby enhancing the fluid motion in the transverse direction. This results in a thicker transverse momentum boundary layer. Physically, while faster stretching suppresses streamwise velocity due to increased frictional resistance, it simultaneously amplifies transverse velocity by diverting fluid laterally.

Table 2: Impact of α, γ, ϕ, M on C_{fx} and C_{fy}

CuO-(EG-Water)-nanofluid						TiO_2-(EG-Water)-nanofluid	
α	γ	ϕ	M	$-C_{fx}$	$-C_{fy}$	$-C_{fx}$	$-C_{fy}$
1.5	0.2	0.01	0.2	2.55445678	4.98433684	2.53032326	4.93560711
1.6				2.58738346	5.37972031	2.56289921	5.32709948
1.7				2.61982909	5.78516507	2.59499958	5.72854772
	0.3			2.38330305	6.00179877	2.36092715	5.94283163
	0.4			2.16653674	6.21899535	2.14639054	6.15768988
	0.5			1.96695671	6.43483374	1.94884402	6.37122250
		0.02		2.03572193	6.67011788	1.99966366	6.54364079
		0.03		2.10527272	6.90778164	2.05139587	6.71903436
		0.04		2.17568853	7.14812292	2.10523572	6.89755173
			0.4	2.25990603	7.21789465	2.19122175	6.97000615
			0.8	2.42331215	7.35953983	2.35993956	7.11717882
			1.2	2.58022435	7.50315114	2.52140764	7.26638930

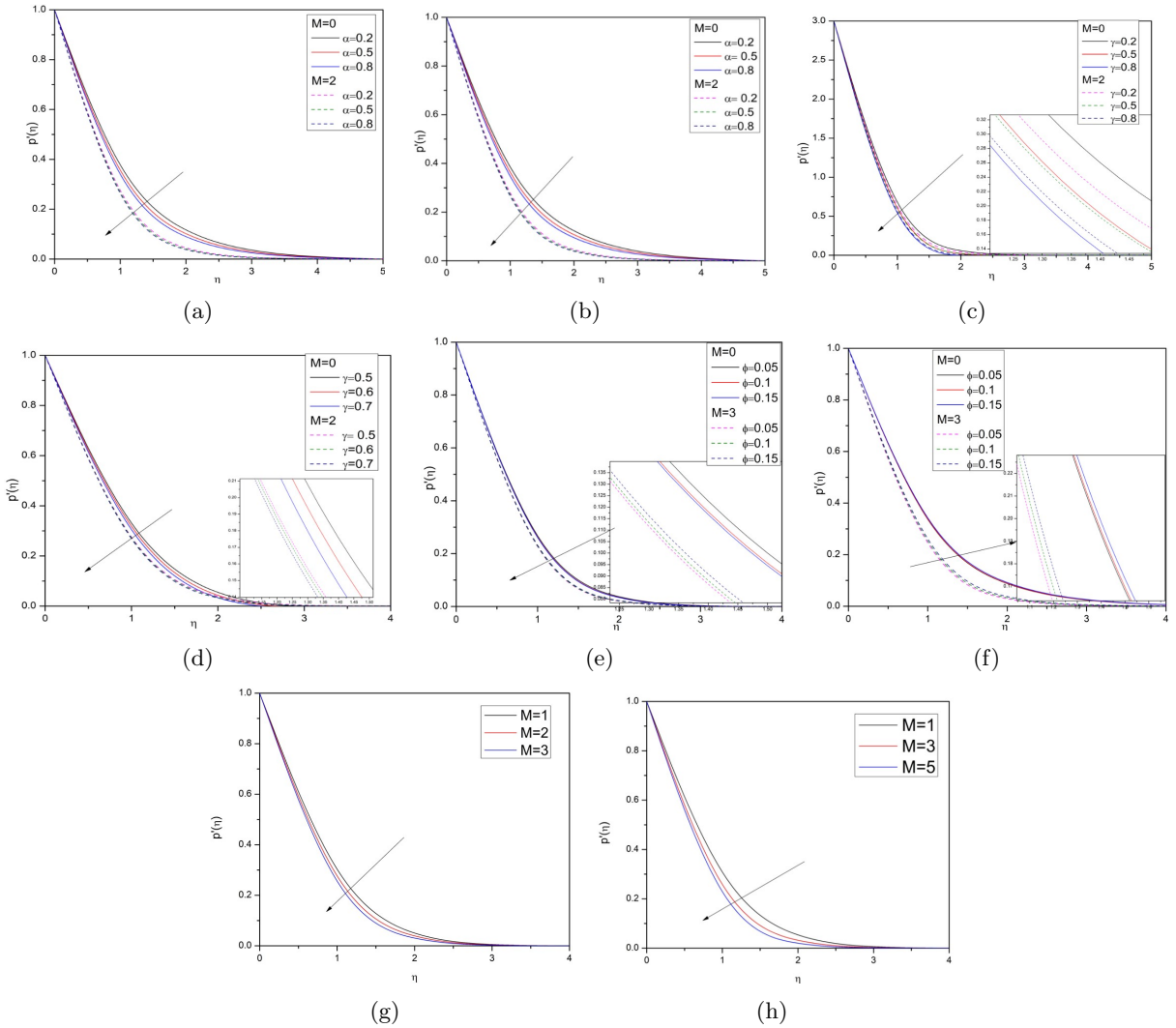

Figure 2: Influence of various α, various rotation parameter γ, volume fraction ϕ and Magnetic parameter M on velocity $p\prime(\eta)$ for CuO hybrid base fluid and TiO_2 hybrid base fluid of nanoparticles.

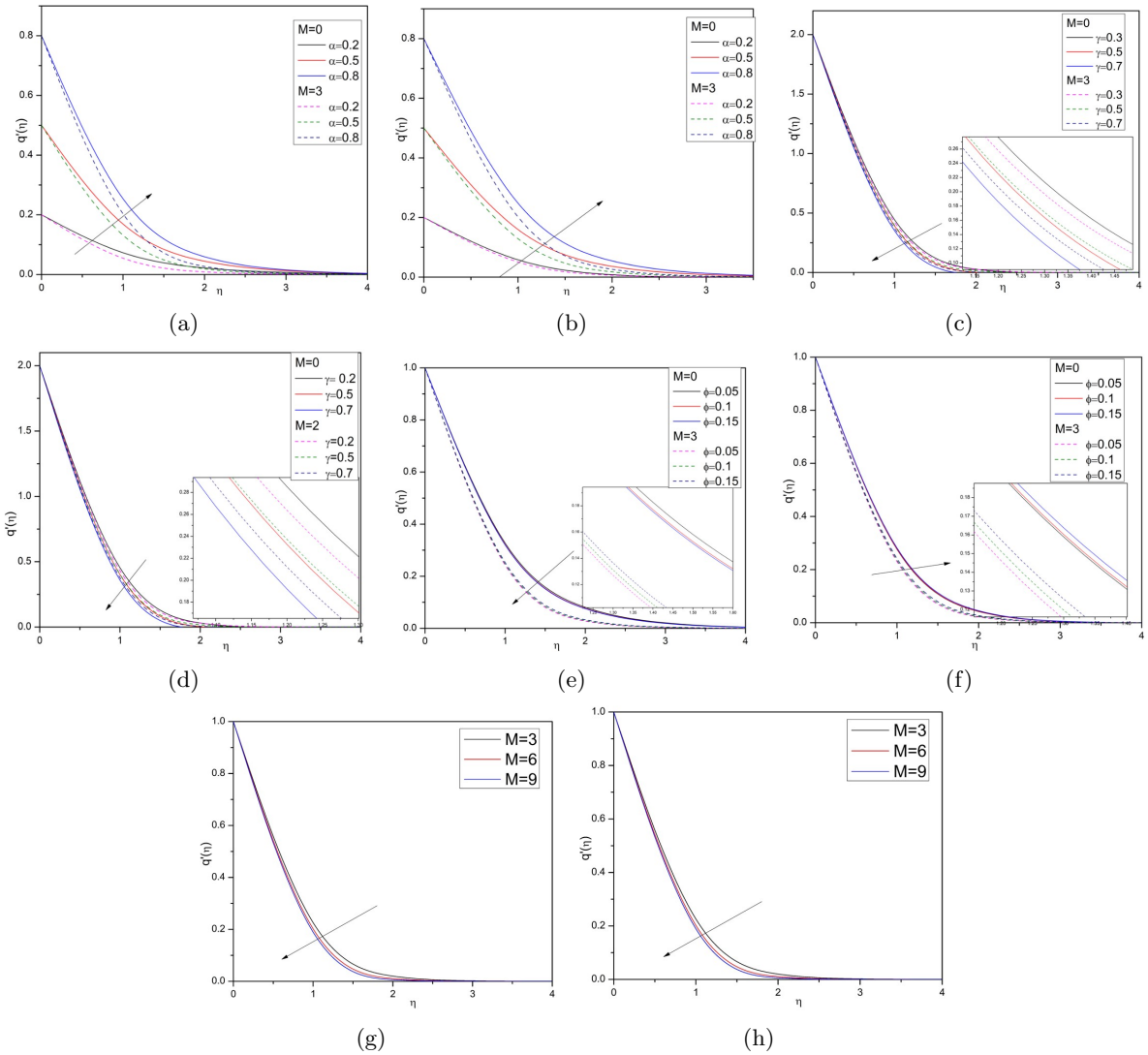

Figure 3: Influence of stretching ratio parameter α, rotation parameter γ, volume fraction ϕ and Magnetic parameter M on velocity $q\prime(\eta)$ for CuO hybrid base fluid and TiO_2 hybrid base fluid of nanoparticles.

The rotation parameter γ plays a crucial role in modifying the momentum transport due to the presence of Coriolis forces as shown in Figure (2c-2d) and (3c-3d). As γ increases, both the streamwise and transverse velocity components are suppressed. Physically, this represents the Coriolis force which acts perpendicular to the direction of motion, diverting momentum and thereby reducing the effective velocity in both directions. This deflecting action enhances resistance within the fluid, which limits the penetration of velocity into the boundary layer. As a result, the streamwise velocity profile decays more sharply, while the transverse velocity also weakens due to rotational damping. The overall effect is a reduction in both velocity boundary layer thicknesses, reflecting the stabilizing influence of system rotation on fluid motion. This gives the understanding of rotational damping of velocity and heat transfer is vital in rotating machinery, turbine cooling, and geophysical flows, where Coriolis forces influence fluid stability.

When the magnetic field interacts with the electrically conducting hybrid nanofluid, the magnetic parameter M incorporates Lorentz forces. The effect of M on axial and transverse direction is as depicted in the figure (2g-2h), (3g) and (3h). The Magnetic parameter M physically represents the square root of the ration of Lorentz force to Viscous force. With increasing M, both streamwise and transverse velocity

profiles are reduced. The Lorentz force counteracts the fluid motion, functioning as a resistive drag. The attenuation of velocity becomes increasingly evident at elevated M values, where momentum diffusion is offset by magnetic resistance. Consequently, the velocity boundary layer becomes thinner, indicating that the magnetic field inhibits fluid motion and stabilizes the flow. Physically, the application of a magnetic field provides an additional controlling mechanism for regulating velocity in electrically conducting fluids, although it also results in higher energy losses due to resistive heating. The control of flow resistance and heat retention by magnetic fields is essential in MHD power generation, electromagnetic pumps, and cooling of nuclear reactors.

The nanoparticle volume fraction ϕ influences velocity through its impact on the effective viscosity and density of the hybrid nanofluid and its effect on the fluid flow is as illustrated as shown in Figure (3e,3f) and Figure (4e,4f). An increase in ϕ corresponds to a greater concentration of nanoparticles suspended in the base fluid, which enhances the effective viscosity. As a result, both streamwise and transverse velocity components exhibit a decreasing trend with higher ϕ. The denser, more viscous hybrid nanofluid experiences stronger internal resistance, leading to greater momentum dissipation and reduced velocity magnitudes. This behaviour reflects the fact that, although hybrid nanofluids enhance thermal transport, their momentum response is weakened due to the added resistance from suspended nanoparticles. Consequently, the momentum boundary layer becomes thinner with increasing nanoparticle concentration. Thereby, tuning nanoparticle concentration provides design flexibility for microchannel heat sinks, biomedical cooling systems, and advanced thermal management technologies.

Table 3: Impact of A, M, ϕ and Ec on Nu_x

				CuO-(EG-Water)-nanofluid	TiO_2-(EG-Water)-nanofluid
A	M	ϕ	Ec	Nu_x	
0.2	0.4	0.01	0.1	-0.05897403	-0.056434652
0.3				0.066900092	0.069219247
0.4				0.175524957	0.177657192
0.5				0.270316871	0.272288663
	0.6			0.230616005	0.232375547
	0.8			0.191591004	0.193153944
	1			0.153201841	0.154582094
	1.2			0.115410211	0.116620141
		0.02		0.085536524	0.088002255
		0.03		0.055371416	0.0591346
		0.04		0.024915998	0.03001446
			0.3	-0.373949436	-0.376573648
			0.5	-0.772814871	-0.783161758
			0.7	-1.17168031	-1.18974987

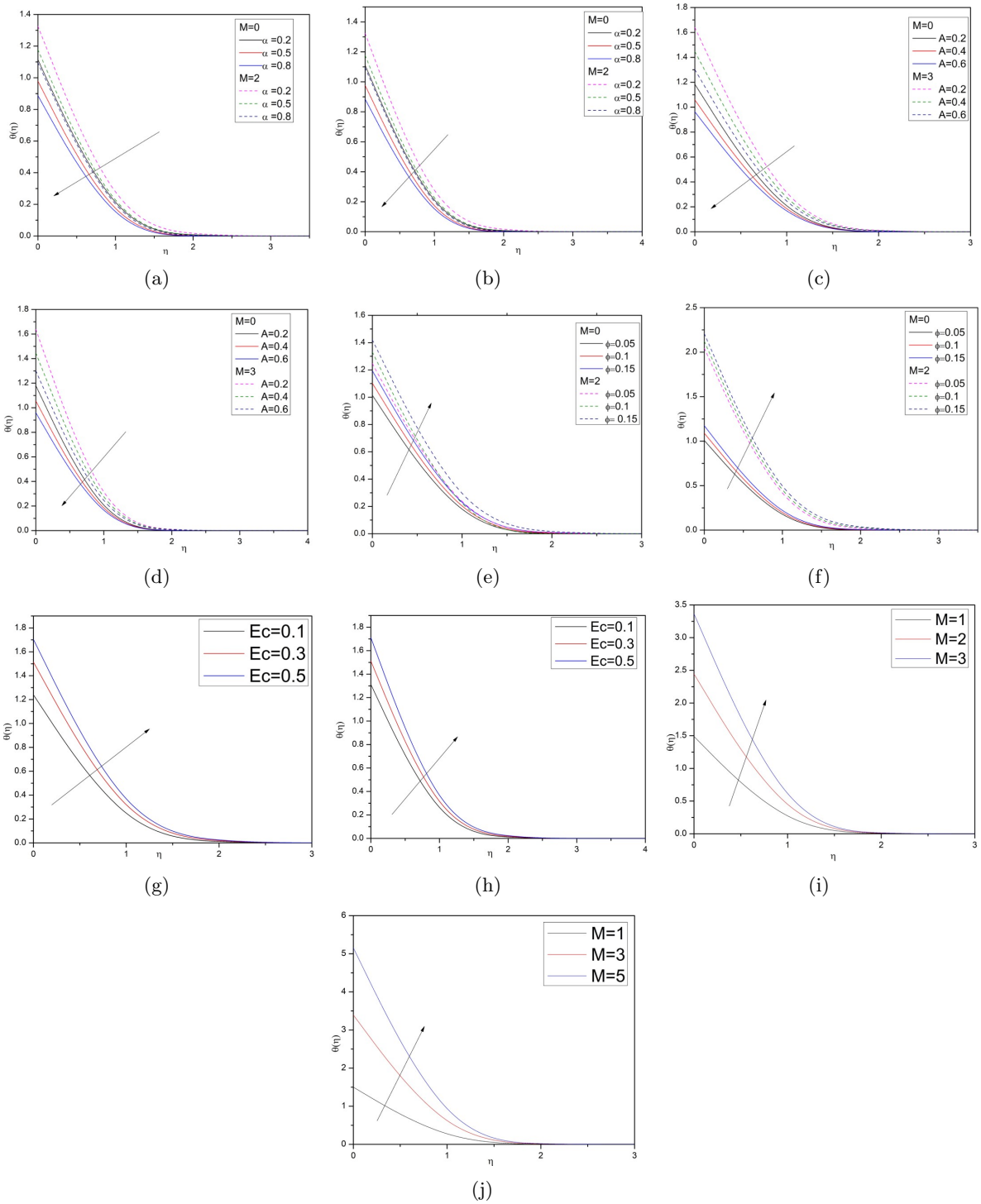

Figure 4: Impacts of stretching ratio parameter α, temperature exponent A, volume fraction ϕ, Eckert number Ec and Magnetic parameter M on temperature curve $\theta(\eta)$ for CuO hybrid base fluid and TiO_2 hybrid base fluid of nanoparticles.

The stretching parameter α exerts a pronounced influence on the thermal boundary layer as depicted in the Figures 4a-4b. As α increases, the sheet stretches more rapidly, which enhances the convective

transport of momentum away from the wall. This accelerated stretching reduces the time available for heat to diffuse into the fluid, thereby causing the temperature profile to decrease. Physically, the fluid particles near the wall are pulled faster along the stretching sheet, which promotes stronger cooling of the surface region and results in a thinner thermal boundary layer. Consequently, higher stretching ratios are associated with lower temperature distributions across the boundary layer, indicating improved heat removal efficiency from the surface. The ability to regulate thermal boundary layers via stretching is directly applicable in polymer extrusion and cooling of metallic sheets, where surface stretching controls heat removal efficiency.

The temperature exponent parameter A dictates the exponential distribution of wall temperature along the stretching surface, as defined by $T_w = T_\infty + T_0 e^{\frac{A(x+y)}{2L}}$, The effect of which is as portrayed in the Figures 4c-4d. When A increases, the wall temperature rises more sharply near the surface, creating steeper thermal gradients in the immediate vicinity of the wall. This strong gradient promotes rapid heat diffusion into the nearby fluid layers, but at the same time, it accelerates thermal decay away from the wall. As a result, the temperature field exhibits a diminishing trend in the boundary layer for larger values of A. Physically, a higher temperature exponent intensifies localized heating near the surface, but the fluid is unable to retain this excess energy farther into the boundary layer, leading to reduced overall temperature profiles and a thinner thermal boundary layer. Exponential variation of wall temperature is relevant to thermal processing of materials and fiber-spinning industries, where surface heating is spatially non-uniform.

The nanoparticle volume fraction ϕ directly affects the optimum thermal conductivity of the hybrid nanofluid, as illustrated in figures 4e-4f. As ϕ rises, a greater number of solid particles are scattered in the underlying fluid, hence augmenting its thermal conductivity. Consequently, the temperature profile rises with depletion of ϕ, resulting in a thicker thermal boundary layer. Physically, the suspended nanoparticles act as thermal energy carriers, facilitating faster heat transfer from the heated surface to the surrounding fluid. While this improves heat conduction, it also reduces cooling efficiency since the fluid retains higher thermal energy across the boundary layer.

The Eckert number Ec quantifies the contribution of viscous dissipation to the energy equation. As Ec increases, the conversion of kinetic energy into internal energy through viscous effects becomes more significant. This additional heat generation elevates the temperature of the fluid and causes the thermal boundary layer thickness to expand. Physically, stronger viscous heating offsets convective cooling, leading to higher fluid temperatures throughout the boundary layer. The effect is especially prominent in high-speed stretching flows, where large velocity gradients produce substantial viscous dissipation. Viscous heating effects become significant in high-speed aerospace systems and microfluidic devices, where internal dissipation strongly affects temperature control.

The magnetic parameter M significantly influences the thermal behavior of the hybrid nanofluid as shown in Figures 4i-4j. As M increases, the Lorentz force acts as a resistive drag, suppressing the fluid motion. This reduction in velocity weakens convective transport, permitting enhanced heat accumulation in the boundary layer. Consequently, thermal boundary layer becomes thicker with escalation in temperature profiles which is result of rise in Magnetic parameter M. Physically, the magnetic field acts as a stabilizing mechanism for momentum but simultaneously enhances thermal energy retention in the fluid due to reduced convective cooling. This dual effect highlights the role of magnetic fields in controlling both flow resistance and thermal distribution in electrically conducting hybrid nanofluids.

Table 1 presents the thermophysical properties of the examined nanoparticles. The computational results for Nusselt number and skin friction of copper oxide (CuO) and titanium dioxide (TiO_2) hybrid base fluid, presented in Tables 2 and 3, exhibit unique patterns influenced by particular physical parameters. Table 2 illustrates the influence of the stretching ratio α, nanoparticle volume fraction ϕ, rotation parameter γ and magnetic parameter M on the skin-friction coefficients of $CuO - (EG - Water)$ and $TiO_2 - (EG - Water)$ hybrid nanofluids. An increase in α enhances both streamwise and transverse skin friction, reflecting steeper velocity gradients near the stretching surface. As γ increases, the streamwise skin friction decreases while the transverse component rises, demonstrating momentum redistribution induced by rotational motion. Higher ϕ amplifies both $-Cf_x$ and $-Cf_y$ owing to the rise in effective viscosity and density with nanoparticle loading. Similarly, largrengthens both shear components due to the Lorentz forcThis study examines the steady flow of a rotating hybrid Nano fluid in three-dimensional

plane affected by the temperature exponent and stretching ratio over a surface that expands exponentially in the presence of a magnetic field. The current work contemplates combination of Nano particles such as Copper oxide (CuO) and Titanium dioxide (TiO_2) suspended in an ethylene glycol–water as a base fluid. The transformed nonlinear boundary value problem was solved using the shooting method using Maple. The impact of non-dimensional factors on Nusselt number, temperature, skin friction and velocity was thoroughly examined. The main findings can be summarized as follows: e acting on the boundary layer. Overall, CuO based nanofluids exhibit marginally higher skin-friction values than TiO_2 based nanofluids, although the general trends remain comparable. Table 3 is prepared to find the heat transfer performance of nanofluid through rising A, M,ϕ and Ec. Here, the magnitude of Nusselt quantity falls for both the nanofluids through magnetic parameter, volume fraction and Eckert number while an improvement is visualized through rising temperature exponent.

5. Conclusion

This study examines the steady flow of a rotating hybrid Nano fluid in a three-dimensional plane affected by the temperature exponent and stretching ratio over a surface that expands exponentially in the presence of a magnetic field. The current work contemplates combination of Nano particles such as Copper oxide (CuO) and Titanium dioxide (TiO_2) suspended in an ethylene glycol-water as a base fluid. The transformed nonlinear boundary value problem was solved using the shooting method using Maple. The impact of non-dimensional factors on Nusselt number, temperature, skin friction and velocity was thoroughly examined.

The main findings can be summarized as follows:

- An elevation in the stretching ratio parameter (α) diminishes the stream wise velocity, augments the transverse velocity, concurrently decreases the temperature profile, and narrows the thermal boundary layer.
- The rotation parameter (γ) diminishes both velocity components due to Coriolis effects, while promoting thicker thermal boundary layers.
- A higher magnetic parameter (M) reduces both velocity components as a result of Lorentz force resistance, yet raises the temperature profile by weakening convective cooling.
- Increasing the nanoparticle volume fraction (ϕ) decreases velocity due to enhanced viscosity but elevates temperature distribution owing to improved thermal conductivity.
- The temperature exponent (A) reduces the temperature profile by lowering the effective wall-fluid heat transfer rate, thereby thinning the thermal boundary layer.
- A higher Eckert number (Ec) intensifies viscous dissipation effects, resulting in elevated temperature distributions across the boundary layer.
- The presence of the magnetic field enhances heat transfer resistance, causing depletion in the Nusselt number, while skin-friction coefficients (Cf_x, Cf_y) increase due to stronger velocity gradients at the wall.
- $CuO-(EG-Water)$ and $TiO_2-(EG-Water)$ hybrid nanofluids both demonstrate these trends, but CuO-based hybrid nanofluids exhibit stronger magnetic sensitivity due to higher electrical conductivity.

Overall, the results show that the combined effects of rotation, stretching, magnetic field, and nanoparticle suspension provide an effective mechanism to regulate both momentum and heat transfer in boundary layer flows. These findings are directly relevant to polymer extrusion, cooling of rotating machinery, electromagnetic pumps, MHD power generation, fiber-spinning processes, and microchannel thermal systems, where precise control of velocity and heat transfer is crucial.

Acknowledgments

Authors acknowledge the support from REVA University, SJC Institute of Technology, RAMAIAH Institute of Technology.

References

1. Abbas, S. Z., Khan, W. A., Kadry, S., Khan, M. I., Waqas, M., & Khan, M. I. (2020). *Computer Methods and Programs in Biomedicine*, 190. https://doi.org/10.1016/j.cmpb.2020.105363

2. Anwar, M. S., Khan, M., Hussain, Z., Muhammad, T., & Puneeth, V. (2025). *Journal of Radiation Research and Applied Sciences*, 18(1), 101240. https://doi.org/10.1016/j.jrras.2024.101240

3. Choi, S. U. and J. A. E. (1995). *Argonne National Lab.(ANL), Argonne, IL (United States).*

4. Javed, T., Sajid, M., Abbas, Z., & Ali, N. (2011). *International Journal of Numerical Methods for Heat and Fluid Flow*, 21(7), 903–908. https://doi.org/10.1108/09615531111162855

5. Kumari, M., Grosan, T., & Pop, I. (2006). *Rotating Flow of Power-Law Fluids over a Stretching Surface* (Vol. 26, Issue 1).

6. Madiha Takreem, K., Venkateswarlu, B., Misra, A., Satya Narayana, P. V., & Harish Babu, D. (2025). *Journal of Thermal Analysis and Calorimetry*, 150(3), 2133–2149. https://doi.org/10.1007/s10973-024-13840-y

7. Mahmood, Z., Alhazmi, S. E., Alhowaity, A., Marzouki, R., Al-Ansari, N., & Khan, U. (2022). *Scientific Reports*, 12(1). https://doi.org/10.1038/s41598-022-20074-1

8. Marzougui, S., Mebarek-Oudina, F., Assia, A., Magherbi, M., Shah, Z., & Ramesh, K. (2021). *Journal of Thermal Analysis and Calorimetry*, 143(3), 2203–2214. https://doi.org/10.1007/s10973-020-09662-3

9. Nabwey, H. A., EL-Hakiem, A. M. A., Khan, W. A., Abdelrahman, Z. M., Rashad, A. M., & Hawsah, M. A. (2024). *Chemical Engineering Journal Advances*, 18. https://doi.org/10.1016/j.ceja.2024.100604

10. Rafique, K., Mahmood, Z., Adnan, Khan, U., Muhammad, T., El-Rahman, M. A., Bajri, S. A., & Khalifa, H. A. E. W. (2024). *Journal of Computational Design and Engineering*, 11(2), 146–160. https://doi.org/10.1093/jcde/qwae029

11. Rashid, A., Ayaz, M., & Islam, S. (2023). *Advances in Mechanical Engineering*, 15(6). https://doi.org/10.1177/16878132231179611

12. Reddy, B. S., and Naik, S. H. S. (2024). *Partial Differential Equations in Applied Mathematics*, 11. https://doi.org/10.1016/j.padiff.2024.100790

13. Rosali, H., Ishak, A., Nazar, R., & Pop, I. (2015). *Journal of Molecular Liquids*, 211, 965-969. https://doi.org/10.1016/j.molliq.2015.08.026

14. Takhar, H. S., & Nath, G. (1998). *In Z. angew. Math. Phys* (Vol. 49).

15. Thumma, T., Bég, O. A., & Sheri, S. R. (2017). *Proceedings of the Institution of Mechanical Engineers, Part N: Journal of Nanomaterials, Nanoengineering and Nanosystems*, 231(4), 179-194. https://doi.org/10.1177/2397791417731452

16. Thumma, T., & Mishra, S. R. (2018). *Journal of Nanofluids*, 7(3), 516-526. https://doi.org/10.1166/jon.2018.1469

17. Thumma, T., & Mishra, S. R. (2020). *Journal of Computational Design and Engineering*, 7(4), 412-426. https://doi.org/10.1093/jcde/qwaa034

18. Thumma, T., & Satya, S. N. (2023). *Australian Journal of Mechanical Engineering*, 21(1), 221-233. https://doi.org/10.1080/14484846.2020.1842158

19. Thumma, T., Wakif, A., & Animasaun, I. L. (2020). *Heat Transfer*, 49(5), 2595–2626. https://doi.org/10.1002/htj.21736

20. Wakif, A., Chamkha, A., Thumma, T., Animasaun, I. L., & Sehaqui, R. (2021). *Journal of Thermal Analysis and Calorimetry*, 143(2), 1201-1220. https://doi.org/10.1007/s10973-020-09488-z

21. Wang, C. Y. (1988). *In Journal of Applied Mathematics and Physics (ZAMP)* (Vol. 39).

22. Zaimi, K., Ishak, A., & Pop, I. (2013). *Applied Mathematics and Mechanics (English Edition)*, 34(8), 945–952. https://doi.org/10.1007/s10483-013-1719-9

Nomenclature

A	temperature exponent parameter	∞	condition at free steam
q_w	wall heat flux $[Wm^{-2}]$	w	condition at wall
$c_{fx},\ c_{fy}$	Skin friction along the x and y-direction	s	solid nano-particles
$u_w,\ v_w$	exponentially stretching velocities at the surface $[ms^{-}1]$	τ_w	viscous stress at the surface $\left[\frac{N}{m^2}\right]$
P_r	Prandtl number	$f,\ nf$	base fluid and nanofluid
Nu_x	Nusselt number	Re_x	local Reynolds number
α_{nf}	thermal diffusivity $\left[\frac{m^2}{s}\right]$ of nanofluid	$u,\ v,\ w$	components of velocity[m/s] in x, y, z-direction. $[ms^{-1}]$
ϕ	nano-particles volume fraction	$T,\ T_\infty,\ T_w$	the temperature of the fluid, ambient temperature, wall temperature $[K]$
θ	dimensionless temperature component	N_c	convective parameter
Ω	constant angular velocity $\left[s^{-1}\right]$	$p.\ q$	dimensionless components of velocity
Ec	Eckert number	u_o, v_o	rates of stretching $[s^{-}1]$
M	Magnetic parameter	u_w, v_w	exponentially stretching velocities at the surface $[m/s]$
$\sigma_f,\ \ \sigma_{nf}$	Electrical conductance $\left[\frac{s}{m}\right]$ of the base fluid and nanofluid respectively	v_f, v_{nf}	kinematic viscosities $\left[\frac{m^2}{s}\right]$ of the base fluid and nanofluid respectively
μ_f, μ_{nf}	dynamic viscosities $\left[\frac{Nc}{m^2}\right]$ of the base fluid and nanofluid respectively	$\rho_s, \rho_f, \rho_{nf}$	density $\left[\frac{Kg}{m^3}\right]$ of solid nanoparticles, base fluid, and nanofluid respectively
k_s, k_f, k_{nf}	thermal conductivities $\left[\frac{W}{mK}\right]$ of solid nanoparticles, base fluid, and nanofluid	$(c_p)_f, (c_p)_{nf}$	: volumetric heat capacity $\left[\frac{J}{Kg.K}\right]$ of base fluid and nano fluid respectively Subscripts

Mahesh Venugopalreddy,
https://orcid.org/0009-0003-1646-0925?lang=en
Department of Mathematics,
SJC Institute of technology
Chikkaballapur,
Karnataka, India.
E-mail address: mahi4mgangi@gmail.com

and

Sreegowrav Konduru Ravikumar,*
https://orcid.org/0000-0003-2069-8402
Department of Mathematics,
School of Applied Sciences,
REVA University
Bengaluru
Karnataka,
India.
E-mail address: gowrav.86@gmail.com

and

Dinesh Pobbathy Aswathanarayana Setty,
https://orcid.org/0000-0002-7698-6705
Department of Mathematics,
Ramaiah Institute of Technology (Affiliated to Visvesveraya Technological University),
Bengaluru
Karnataka,
India.
E-mail address: dineshdpa@msrit.edu

and

Sibyala Vijayakumar Varma,
https://orcid.org/0000-0002-9757-9316,
REVA Research Centre,
REVA University
Bengaluru
Karnataka,

India.
E-mail address: vijayakumar.varma@reva.edu.in